PHOTOMETRIC AND ATMOSPHERIC CORRECTION OF CASSIS IMAGES. S. Douté[1], G. Munaretto[2], L. Tornabene[3], M. Pajola[2], and A. Lucchetti[2]. [1]Université Grenoble Alpes, CNRS, Institut de Planétologie et d'Astrophysique de Grenoble (IPAG), France, (sylvain.doute@univ-grenoble-alpes.fr), [2]Astronomical Observatory of Padova (OAPD), INAF, Italy, [3]Inst. Earth & Space Exploration, Earth Sci., Western University, London, Canada.

Introduction: The Colour and Stereo Surface Imaging System (CaSSIS) [1] is the surface imaging instrument on the European Space Agency/Roscosmos ExoMars Trace Gas Orbiter (TGO), which was launched to Mars in March 2016 and began nominal science operations in April 2018. CaSSIS offers advanced colour and stereo imaging capabilities with the ability to acquire multispectral images both in front and behind the TGO during a single orbit. The acquisition is performed in four spectral channels -BLU, NIR, RED and PAN - allowing an improved discrimination among surface materials, particularly minerals containing ferrous and ferric iron. However, the spectral radiance measured by remote sensing instrument orbiting Mars is significantly influenced by the gaseous absorptions and aerosol scattering by airborne ferric iron oxide dust and water ice. This influences the apparent photometry and spectral signatures coming from the surface and impacts the ability to derive higher-level data products related to surface properties such as band ratios, spectral indices, and albedo maps.

In this contribution, we present an experiment aimed at correcting the atmospheric and photometric effects affecting the CaSSIS image MY35_013826_196 acquired at $L_S = 339°$, MY 35 over the Columbia Hills of Gusev crater, i.e. where the Spirit rover made in situ exploration. The processing, which also leads to an estimation of the atmospheric opacity (AOD), relies on a Digital Terrain Model (DTM), a CRISM derived reflectance model of the scene, and a series of image simulations. The added value of the correction is assessed qualitatively by comparing the original and corrected images as well as the corresponding Colour Band Ratio Composites CBRC1 proposed by [2]. The corrected image is also being used to validate the dark subtraction method, which is a simple empirical correction that shows some promise for minimizing the scattering effects of the atmosphere and isolating the surface component [Tornabene et al. 2021 LPSC; this conference].

Data: A photogrammetrically generated CTX DTM has been densified at 6 m/pixel (comparable to CaSSIS 4.6 m/pixel) according to [3] and has been co-registered with the CaSSIS image. The simulation is based on this topographical scene that is covered uniformly with a reference material described by a BRDF parametric model (RTLS) expressed at 91 wavelengths from 0.4-1.1 μm (i.e., the spectral sensitivity range of CaSSIS). The model ρ_{model} is extracted from the processing of the CRISM EPF observation FRT3192 of the Columbia Hills [4] and corresponds to the bright reddish end member (dust dominated terrains). A simulation tool [5] is used to compute image cubes of atmospheric radiative transfer quantities and a realistic Bottom-Of-Atmosphere (BOA) simulated image. The latter corresponds to the real CaSSIS illumination and viewing conditions (SZA=60.48°, VZA=10.5°, phase=60.55°) and expresses the upward radiance reflected by the surface under different irradiance terms (direct, diffuse, and reflected by the neighbouring facets). The calculation is performed for all wavelengths and the resulting products (direct and diffuse transmission through the atmosphere G_d, path radiance R_d, and BOA image boa_ref_image) are convolved by the spectral response function for each channel of the CaSSIS sensor. Since we do not know the AOD of the atmosphere at the moment of the acquisition, we try to obtain an estimate from the image itself. For that purpose we will consider a series of 21 AOD values regularly distributed in [0.1-1.5], each value leading to a set of radiative transfer products and BOA images to seek the best match to the actual CaSSIS imgage, and thereby constrain the best estimate for the AOD.

Aerosol optical depth estimation and correction of the CaSSIS image: For each AOD, a model of the CaSSIS Top-Of-Atmosphere TOA image is built, $toa\_ref\_image = boa\_ref\_image * G_d + R_d$, that we can compare to the real image (toa_real_image). A vector of multiplicative calibration factors is then estimated by taking the mean of the image ratio $\beta = \textbf{mean}\,(toa\_real\_image/toa\_ref\_image)$ for each CaSSIS channel. These factors should account for any global radiometric mismatch between the real image and the simulation. Once the calibration factors are known, we can subtract the path radiance multiplied by these factors from the real TOA image. In addition, we divide the result by the total atmospheric transmission to get an evaluation of the BOA image:

$$boa\_real\_image = (toa\_real\_image - \beta R_d)/G_d$$

A photometric normalisation is performed by (i) dividing the latter by the reference BOA CaSSIS image and (ii) multiplying by a spectrum calculated according to the reference BRDF model expressed for uniform geometrical conditions (SZA=60.48°, VZA=10.5°, phase=60.55°):

$$normalized\_image = boa\_real\_image/boa\_ref\_image * \rho_{model}$$

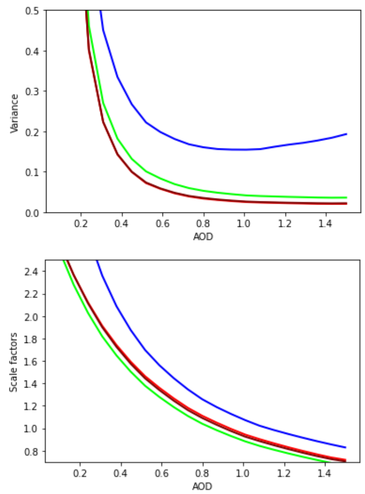

Figure 1: Evolution of the characteristics of the normalised image as a function of the AOD value (blue: BLU filter, green: PAN, red: RED, dark RED: NIR). Top: the amount of residual shading in the image. Bottom: calibration factors β.

Finally, as an indication of the residual shading in the normalised image, we calculate the spatial variance for each channel. We perform the previous steps for each possible value of AOD. As a result, curves of variance as a function of AOD are plotted.

In Fig. 1 (top) we note a strong decrease of variance for each channel until AOD $\approx$ 0.9-1.0. Then the PAN, RED, and NIR variances level off whereas the blue variance starts to increase. We estimate that the minimum of the BLU variance curve that corresponds to minimum shading in the image for this wavelength is indicative of the real AOD that can then be roughly estimated : AOD=1.0 $\pm$ 0.2. Plotting the calibration factors as a function of the AOD value is also very informative. Indeed in Fig. 1 (bottom) we note a monotonous decrease of the factors regardless of the channel from $\approx$ 2.5 to 0.8. Interestingly the curves cross the level 1.0 for 0.9-1.2 which is close to the AOD range estimated from the variance. Consequently we propose a rough estimate AOD $\approx$ 0.9, which is compatible with the climatology of [6]. This value of AOD is used for the final photometric and atmospheric correction of the image according to the equations of this section.

Discussion: Fig. 2 demonstrates that, compared to the TOA image, shading/illumination effects are minimised in the corrected image and the colour variations of the scene are generally enhanced, especially in areas once heavily shadowed or illuminated.

The Colour Band Ratio Composite CBRC1 is also generated for the TOA and corrected CaSSIS images.

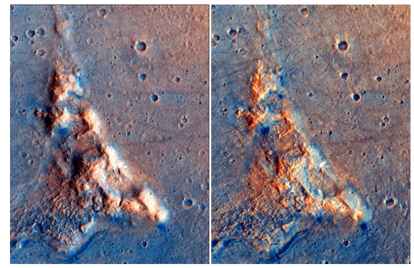

Figure 2: Comparison of two false color versions of CaSSIS image MY35_013826_196 (restricted here to the Columbia hills). Left: original. Right: corrected for photometric and atmospheric effects.

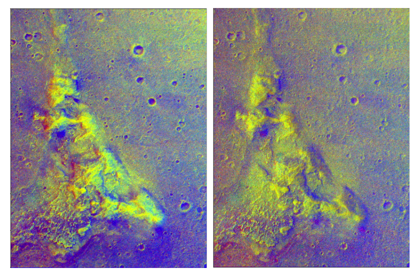

Figure 3: CBRC1 product. Left: from the original image. Right: from the corrected image

Different classes of minerals are expressed by different hues: green-yellow: ferric oxydes (Martian dust), blue: pyroxenes (basaltic sand), red: low contrast or non-Fe-bearing materials [2].

In Fig. 3 the comparison shows that both products shows globally the same spatial distribution of the minerals for the Columbia hills. However, the corrected image has clearly less artefacts, like the reddish hues in the TOA CBRC1 image that correlate with shadows where the atmospheric contribution is the highest. Our method for correcting the atmospheric and photometric effects will be tested in the near future for a scene that shows a higher mineral diversity and will be pivotal for performing quantitative photometric analysis of the surface of Mars.

References: **[1]** N. Thomas et al. In: *Space Science Reviews* 212.3 (Nov. 2017), pp. 1897–1944. ISSN: 1572-9672. **[2]** Livio L. Tornabene et al. In: *Space Science Reviews* 214.1 (Dec. 2017), p. 18. ISSN: 1572-9672. **[3]** Sylvain Doute and Cheng Jiang. In: *IEEE Transactions on Geoscience and Remote Sensing* 58.1 (Jan. 2020), pp. 447–460. **[4]** J. Fernando et al. In: *Icarus* 253 (June 2015), pp. 271–295. **[5]** S. Douté. "Simulating hyperspectral images for Martian 3D scenes." In: *European Planetary Science Congress*. Sept. 2017, EPSC2017–426. **[6]** L. Montabone et al. In: *Icarus* 251 (May 2015), pp. 65–95.